Chemistry of Metals and Alloys

Chem. Met. Alloys 8 (2015) 22-26
Ivan Franko National University of Lviv
www.chemetal-journal.org

The $Ag_2S–Ga_2S_3–As_2S_3$ system

T.L. KLYMUK[1]*, I.D. OLEKSEYUK[1], I.I. MAZURETS'[1]

[1] *Department of Inorganic and Physical Chemistry, Lesya Ukrainka Eastern European National University, Voli Ave. 13, 43025 Lutsk, Ukraine*
* *Corresponding author. Tel.: + 380 95 5293296; e-mail: tamara-klimuk@rambler.ru*

Received March 26, 2015; accepted June 24, 2015; available on-line September 1, 2015

The $Ag_2S–Ga_2S_3–As_2S_3$ system was investigated by differential thermal and X-ray diffraction. The phase diagrams of the systems $Ag_2S–As_2S_3$, $Ag_9GaS_6–Ag_3AsS_3$, $AgGaS_2–AgAsS_2$, and $AgGaS_2–Ag_3AsS_3$ were constructed, as well as the liquidus surface projection and the isothermal section at 500 K. The interaction in the $Ag_2S–As_2S_3$ system is eutectic and is described by the equations $L_{e1} \leftrightarrow Ag_2S + Ag_3AsS_3$ (e_1: 25 mol.% As_2S_3, 720 K), $L_{e2} \leftrightarrow AgAsS_2 + Ag_3AsS_3$ (e_2: 40 mol.% As_2S_3, 650 K), and $L_{e3} \leftrightarrow AgAsS_2 + As_2S_3$ (e_3: >99 mol.% As_2S_3, 580 K). The eutectic point in the $AgGaS_2–AgAsS_2$ system lies at 94 mol.% $AgAsS_2$, 653 K. The coordinates of the eutectic in the $AgGaS_2–Ag_3AsS_3$ system are 92 mol.% Ag_3AsS_3, 670 K, and in the $Ag_9GaS_6–Ag_3AsS_3$ system the eutectic lies at 90 mol.% Ag_3AsS_3, 687 K.

Phase diagram / Isothermal section / Liquidus surface projection

Introduction

The binary and ternary compounds in the system $Ag_2S–Ga_2S_3–As_2S_3$ possess non-linear optical, acousto-optical, photoelectric, luminescent, and other properties. The silver thiogallate $AgGaS_2$ belongs to a class of ternary chalcogenides with the chalcopyrite structure. It exhibits high double refraction and a wide transparency region, and is therefore a promising material for quantum electronics [1]. The ternary compounds Ag_3AsS_3 and $AgAsS_2$ are used as non-linear optical materials [2,3]. As_2S_3 is a glass-forming compound, and therefore glassy materials should exist in the $Ag_2S–Ga_2S_3–As_2S_3$ system.

Three compounds, $AgGaS_2$, Ag_9GaS_6, and $Ag_2Ga_{20}S_{31}$, form in the $Ag_2S–Ga_2S_3$ system [4-7]. $Ag_2Ga_{20}S_{31}$ forms by a peritectic reaction $L + Ga_2S_3 \leftrightarrow Ag_2Ga_{20}S_{31}$ at 1268 K, and has a polymorphous transition at 298 K. $AgGaS_2$ and Ag_9GaS_6 melt congruently at 1273 K and 1063 K, respectively. Ag_9GaS_6 has a polymorphous transition at 308 K. The phase diagram of the $Ag_2S–As_2S_3$ system has been investigated in the range 0-50 mol.% As_2S_3 [8]. Two ternary compounds, Ag_3AsS_3 and $AgAsS_2$, exist in the system [8-10] and melt congruently at 689 K and 753 K, respectively. According to [11], a glass-formation region was found in the range 100-10 mol.% As_2S_3 of the quasi-binary system $Ag_2S–As_2S_3$ under the conditions of extremely rapid quenching (cooling rate ~10^6 K/s).

The phase diagram of the $As_2S_3–Ga_2S_3$ system was investigated in [12]. No ternary compounds were found, and the sub-solidus region features only the crystallization of the solid solutions of LT-Ga_2S_3 and As_2S_3.

Experimental

High-purity elements (silver 99.999 mass%, gallium 99.9997 mass%, sulfur 99.997 mass%) and previously synthesized As_2S_3 (arsenic 99.999 mass%) were used for the synthesis.

All the samples were synthesized in evacuated quartz ampoules with the use of vibration mixing. The temperature in the furnace was raised at a rate of 20-30 K/h to 1100-1200 K. The melts were kept at the maximum temperature for 6 h. The alloys were cooled at the rate of 10-20 K/h to 500 K, and annealed for 600 h to achieve equilibrium state. After annealing, the ampoules were quenched to room temperature into a saturated NaCl solution.

The obtained alloys were investigated by differential thermal analysis (DTA) and X-ray diffraction (XRD). DTA was performed with a set-up consisting of a Thermodent furnace, PDA-1 XY-recorder, and a thermocouple amplifier block. The temperature was controlled by a Pt/Pt-Rh thermocouple. Uniform heating of the furnace was programmed at the rate of 10 K/min, with inertial cooling. Powder diffraction patterns were recorded on

a DRON 4-13 diffractometer with CuK_α-radiation in the 10-80° 2θ range, with 0.05° scan step and 1 s exposure at each point. Powder Cell 2.3 software was used for the X-ray phase analysis.

Results and discussion

As the Ag_2S–As_2S_3 phase diagram had only been investigated in the range 0-50 mol.% As_2S_3 [8], a re-investigation of the system covering the entire concentration range was performed (Fig. 1). The existence of the two ternary compounds, Ag_3AsS_3 and $AgAsS_2$, which both melt congruently, was confirmed. The interaction of the components and the ternary compounds is described by the following equations: $L_{e1} \leftrightarrow Ag_2S + Ag_3AsS_3$ (e_1 = 25 mol.% As_2S_3, 720 K), $L_{e2} \leftrightarrow AgAsS_2 + Ag_3AsS_3$ (e_2 = 40 mol.% As_2S_3, 650 K), and $L_{e3} \leftrightarrow AgAsS_2 + As_2S_3$ (580 K). The temperature of the latter process is only slightly lower than the melting point of As_2S_3 (583 K), therefore this eutectic is degenerate.

The phase diagram of the $AgGaS_2$–$AgAsS_2$ section was investigated in the entire concentration range (Fig. 2).

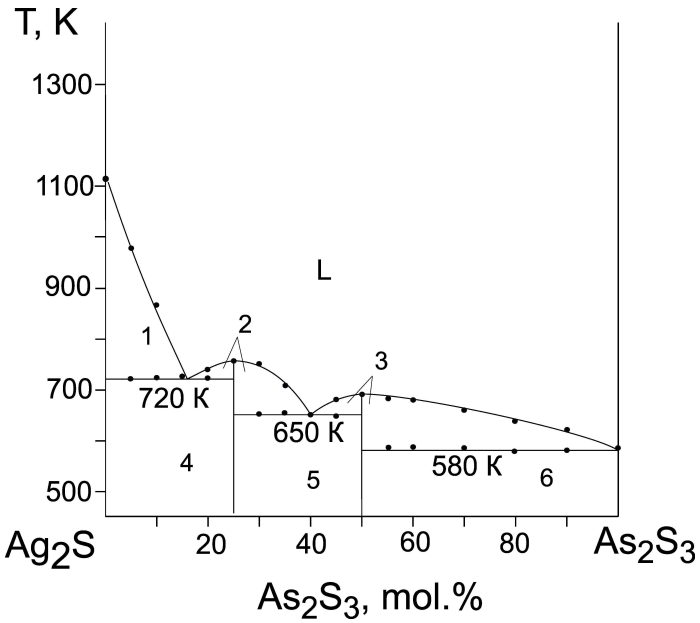

Fig. 1 Phase diagram of the Ag_2S–As_2S_3 system.

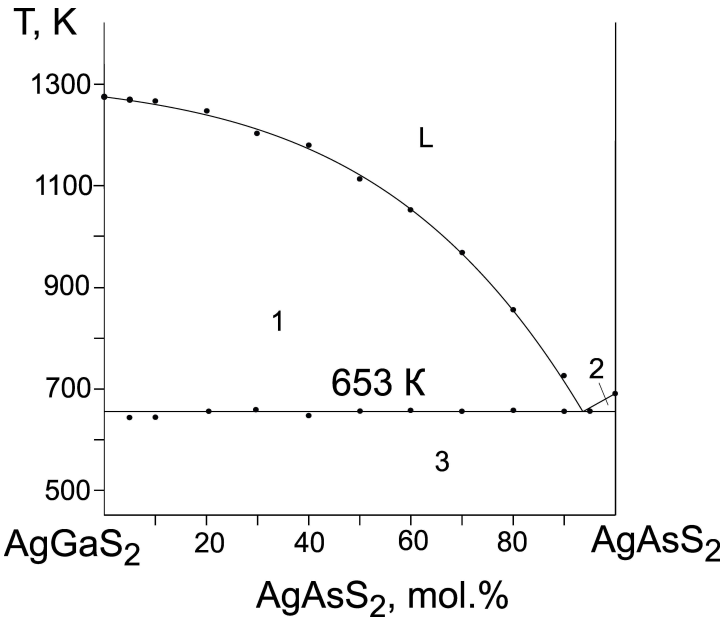

Fig. 2 Phase diagram of the $AgGaS_2$–$AgAsS_2$ system.

The results show that the system is of the eutectic type. The coordinates of the eutectic, determined by the construction of a Tamman triangle, are 94 mol.% $AgAsS_2$, 653 K. The solid solubility in the components is negligible.

The phase diagrams of the sections $AgGaS_2$–Ag_3AsS_3 and Ag_9GaS_6–Ag_3AsS_3 are similar, since both of them are of the eutectic type. The eutectic coordinates are 92 mol.% Ag_3AsS_3, 670 K for the $AgGaS_2$–Ag_3AsS_3 system, and 90 mol.% Ag_3AsS_3, 687 K for the Ag_9GaS_6–Ag_3AsS_3 system.

The phase diagram of the $Ag_2Ga_{20}S_{31}$–As_2S_3 system (Fig. 3) is quasi-binary in the sub-solidus region. The liquidus line consists of the three curves of primary crystallization of α-Ga_2S_3 (field 2), β-Ga_2S_3 (field 4) and As_2S_3 (field 8). The sub-liquidus part features lines that correspond to the beginning of the secondary crystallization of L + β-Ga_2S_3 + $Ag_2Ga_{20}S_{31}$ (in the peritectic reaction L + β-Ga_2S_3 ↔ $Ag_2Ga_{20}S_{31}$) and L + β-Ga_2S_3 + As_2S_3 (in the eutectic reaction L ↔ β-Ga_2S_3 + As_2S_3). The solid solubility in the components does not exceed 2 mol.%. The solidus is a horizontal line at 579 K, which belongs to the plane of the non-variant peritectic process L + β-Ga_2S_3 ↔ As_2S_3 + $Ag_2Ga_{20}S_{31}$.

The isothermal section of the Ag_2S–Ga_2S_3–As_2S_3 system at 500 K is presented in Fig. 4. All the phases existing at this temperature are in the solid state. No quaternary compounds were found in the system. There are six three-phase fields, separated by five two-phase equilibria.

The liquidus surface projection of the Ag_2S–Ga_2S_3–As_2S_3 system is shown in Fig. 5. The system consists of five sub-systems: Ag_2S–Ag_9GaS_6–Ag_3AsS_3, Ag_9GaS_6–$AgGaS_2$–Ag_3AsS_3, $AgGaS_2$–$AgAsS_2$–Ag_3AsS_3, $AgGaS_2$–$AgAsS_2$–As_2S_3, and $AgGaS_2$–Ga_2S_3–As_2S_3, which may be viewed as independent.

The liquidus of the four sub-systems (except $AgGaS_2$–Ga_2S_3–As_2S_3) consists of the three curves of primary crystallization of the components that form the sub-system. The liquidus of the $AgGaS_2$–Ga_2S_3–As_2S_3 system consists of the five fields of primary crystallization of $AgGaS_2$, α-Ga_2S_3, β-Ga_2S_3, $Ag_2Ga_{20}S_{31}$, and As_2S_3. The temperature of the ternary eutectic E_5 in the $AgGaS_2$–$AgAsS_2$–As_2S_3 sub-system is 577 K, which differs only insignificantly from the eutectics in the systems $AgAsS_2$–As_2S_3 (580 K), $AgGaS_2$–As_2S_3 (582 K), and slightly more from that of the system $AgGaS_2$–$AgAsS_2$ (653 K). Analogous situations are observed for the non-variant points E_4 and P_2. The As_2S_3 content of the non-variant points E_4, E_5, P_2 is 98 mol.% As_2S_3, which complicates the preparation of crystalline samples of this composition and hence the investigation of the phase diagram in this part of the system (see enlargement in Fig. 5).

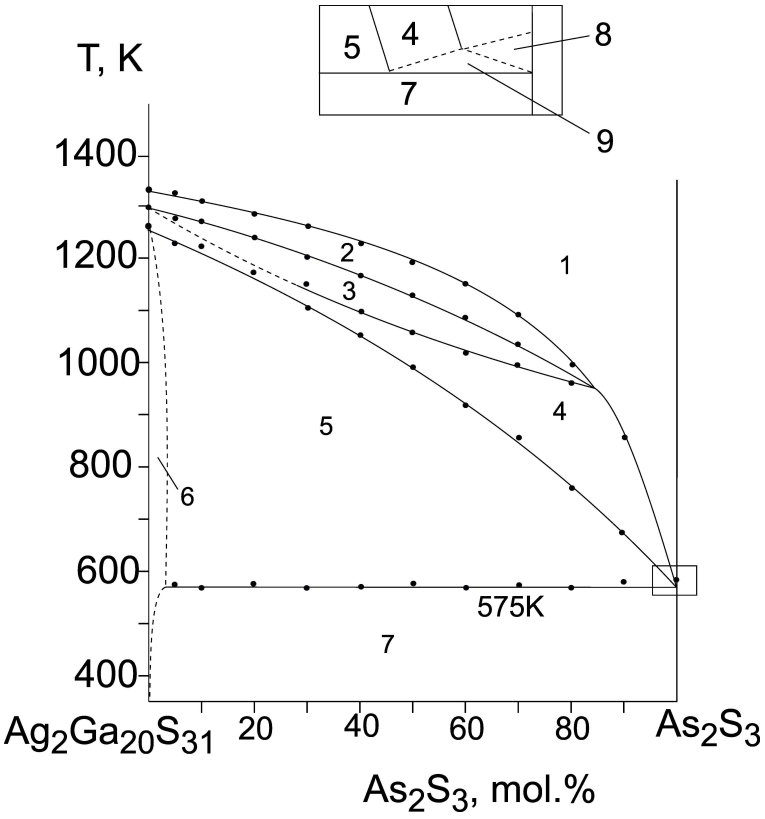

Fig. 3 Phase diagram of the $Ag_2Ga_{20}S_{31}$–As_2S_3 system.

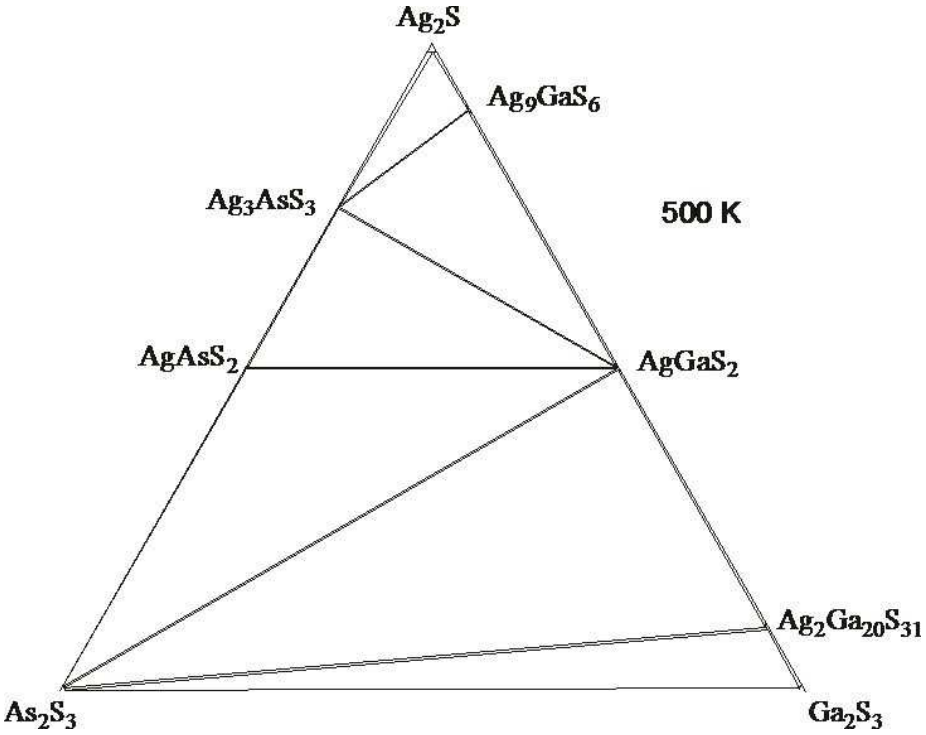

Fig. 4 Isothermal section of the Ag_2S–Ga_2S_3–As_2S_3 system at 500 K.

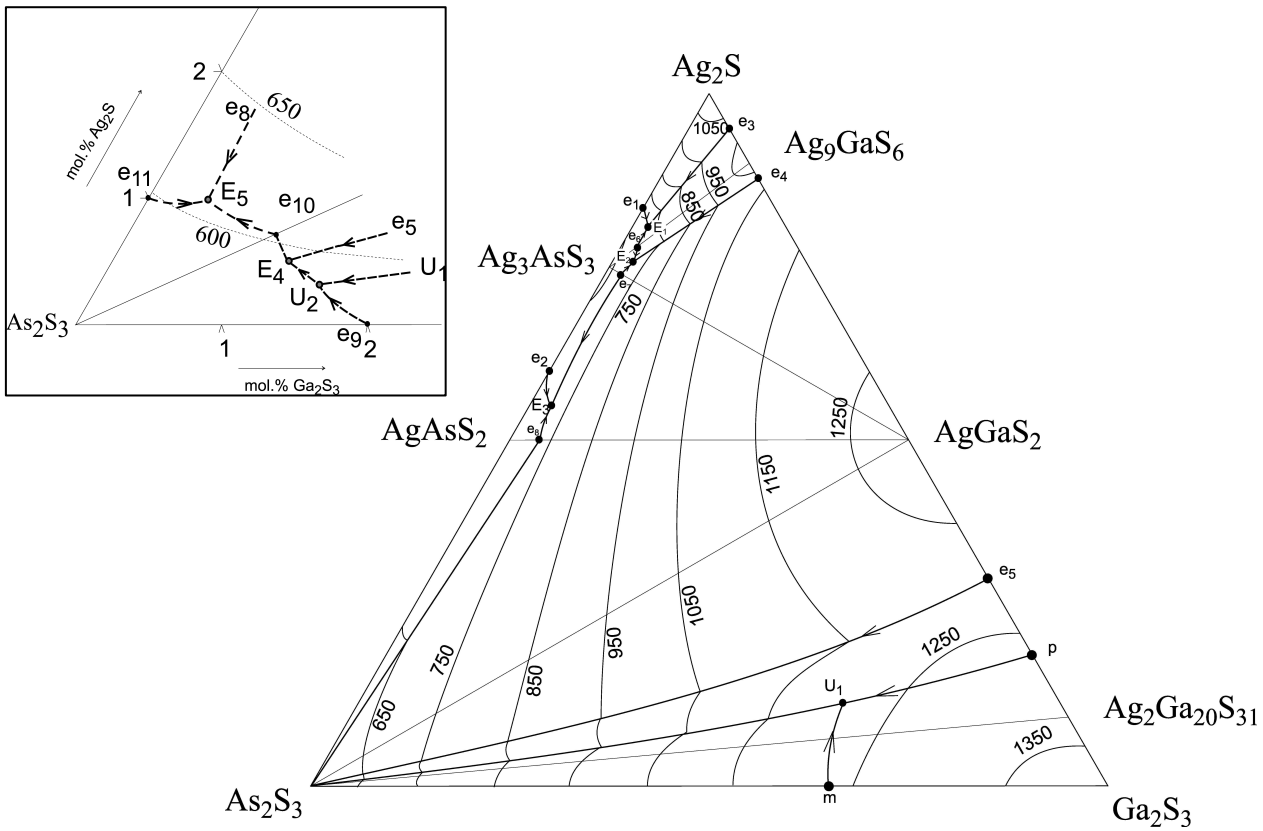

Fig. 5 Liquidus surface projection of the Ag_2S–Ga_2S_3–As_2S_3 system.

Conclusions

Based on the results of X-ray diffraction and differential thermal analysis, we investigated the phase diagrams of the systems $Ag_2S–As_2S_3$, $Ag_9GaS_6–Ag_3AsS_3$, $AgAsS_2–AgGaS_2$, and $AgGaS_2–Ag_3AsS_3$, as well as the liquidus surface projection and the isothermal section at 500 K of the $Ag_2S–Ga_2S_3–As_2S_3$ system. The nature and temperature of the non-variant and monovariant processes were determined.

References

[1] V.V. Badykov, O.V. Skrenbeva, *Kuban State Univ. Bull.* (1982) 124-161.

[2] S.R. Sashital, A.L. Gentile, *J. Cryst. Growth* 69 (1984) 379-387.

[3] I.D. Olekseyuk, *Binary and Ternary Semiconductor Phases in the Systems* $Me–B^V–C^{VI}(D^{VII})$, Vezha, Lutsk, 1995. (In Ukrainian)

[4] G. Brandt, V. Krämer, *Mater. Res. Bull.* 11(11) (1976) 1381-1388.

[5] H. Hahn, G. Frank, W. Klingler, A.D. Meyer, G. Störger, *Z. Anorg. Allg. Chem.* 271(3-4) (1953) 153-170.

[6] S.C. Abrahams, J.L. Bernstein, *J. Chem. Phys.* 59(4) (1973) 1625-1629.

[7] M. Guittard, C. Carcaly, T. Kabré, P.H. Fourcroy, J. Flahaut, *Ann. Chim. (Paris)* 8(3) (1983) 215-225.

[8] F.H. Wehmeier, R.A. Laudise, J.W. Shiever, *Mater. Res. Bull.* 3 (1968) 767-778.

[9] E. Hellner, H. Burzlaff, *Naturwissenschaften* 51 (1964) 35-36.

[10] D. Harker, *J. Chem. Phys.* 4 (1936) 381-390.

[11] Jun Liu, J.J. Videau, B. Tanguy, J. Portier, J.M. Reau, P. Hagenmuller, *Mater. Res. Bull.* 23 (1988)
1315-1320.

[12] T.L. Klymuk, I.I. Mazurets', *Coll. Abstr. VI All-Ukraine Conf. Young Researchers and Students on Modern Challenges in Chemistry*, June 3-6, 2008, Kharkiv, p. 151.